Application of intelligent adaptive force control for a helicopter seat suspension

Mohamad Gohari[a]∗, Mona Tahmasebi[a] , Samaneh Ahmadi,[b]

[a]*Assistant Professor, School of Mechanical Engineering, Arak University of Technology, Arak, Iran*
[b]*MSc Student, Arak University of Technology, Arak, Iran*

A B S T R A C T

The high level of transmitted noise and vibrations of a helicopter flight to the aircrew body can cause discomfort and perhaps affect their performance and physical condition. This paper presents an active seat suspension system with intelligent active force control (AFC) using an artificial neural network (ANN), iterative learning (IL) algorithm, and fuzzy logic (FL) to reduce vibration on the helicopter seat. Therefore, three control schemes are considered for this application, namely AFCANN, AFCIL, and AFCFL. Computer simulations have been performed using MATLAB software to verify the proposed control schemes. The pilot head displacement, acceleration, and also seat acceleration transmissibility are selected as target variables. The simulation results illustrate that the usage of proposed control schemes leads to effective control of target variables, especially active force control using fuzzy logic (AFCFL), which is showing superior performance and accuracy between other intelligent adaptive force control schemes. In future work, this controller will be assessed by experimental tests.

1. Introduction

The excessive interior levels of noise and vibration in helicopters transmitted to the aircrew body are not preventable and happen through flight operations. The high level of severe vibrations leads to anxiety and uneasiness of the aircrew and may affect their health, concentration, and operating performance on flight operations. Thus, the aircrew decision-making can face a

---

∗ Corresponding author:
   E-mail address: moh-gohari@arakut.ac.ir (M. Gohari)

problem in both training and missions. More significantly, long-term exposure may cause occupational damages for the aircrew, such as spine and neck injuries [1]. Consequently, the attenuation of transmitted vibration to the aircrew body is vital to enhance the working environment for the aircrew.

Chen *et al.* reported that some vibration sources in helicopters are internal and aerodynamic loads from the rotor, mechanical vibration from gearboxes, and the highest vibration energy comes from the N/rev harmonics of rotor passage frequency [2]. A number of researchers concentrated on helicopter vibration level suppression and performed some studies on seat suspensions. Two techniques are employed in order to control the helicopter vibrations. The first technique aims to decrease the unsteady aerodynamic loads from the rotor blades to diminish global helicopter body vibrations. For instance, the Individual Blade Control (IBC) [3, 4] and Higher Harmonic Control (HHC)[5] methods have been invented for this issue. The second technique, namely Active Control of Structural Response (ACSR) approach, suppresses the vibration at fuselages such as the cabin or the aircrew seat.

An abrupt method to develop the helicopter ride quality is to propose an adaptive seat to block the vibration transmitted to the aircrew. Presently, passive cushions installed between the aircrew body and the seat structure have been used to decline vibration. These passive systems, as a conventional suspension, include a sprung mass with a constant damping shock absorber to diminish undesired low-frequency vibration. However, they are not adaptive and it is so difficult to optimize them based on various pilot weight and flight configurations. Therefore, semi-active and active suspension systems have been offered by several researchers to install on the seat structure without significant changes in requirement to primary helicopter frames or modification to the rotor and flight control systems. It means that the implementation of an active suspension proposes a feasible solution to decrease the harmful transmitted vibration impacts on aircrew health during operating conditions.

The Magneto-Rheological (MR) and Electro-Rheological (ER) seat suspensions were utilized to reduce vibration in commercial vehicles employing skyhook and sliding mode control algorithms [6-9]. The Lyapunov type robust control was used for the semi-active vibration control of a seat system equipped with a flexible mechanism of a spring and MR fluid damper. Results demonstrate that considering the time delay of the damper successfully reduced the vibration of the seat [10]. Also, the end-stop impact and vibration reduction performance of a seat incorporated with an MR damper were compared to those of the same seat with a conventional damper[11]. Choi and Wereley studied the biodynamic response of the seated human body to sinusoidal vibration and shock loads via seat suspension system implemented to MR dampers, though the findings revealed that the MR dampers significantly attenuate vibration and are not able to suppress shock loads [12]. Hiemenz *et al.* constructed an MR seat suspension system integrated to passive suspension to prepare obvious stiffness at high-frequency excitations[13]. Moreover, Chen *et al.* provide an active seat suspension system utilizing an adaptive force control Law and modal shaker to mitigate the vibration transmission from the helicopter seat to the aircrew[14]. Also, they developed an active suspension system for helicopter seats by applying stacked piezoelectric actuators to perform effective vibration control to the aircrew without the collaboration of the aircrew comfort[15].

Lately, the active control suspensions are supposed to still less practical where the unwanted helicopter vibrations have been regarded as a great restriction for aircrew health. Furthermore,

the conventional control techniques as a simple and relatively stable method could just guarantee acceptable performance at very low-speed operations[16]. New intelligent methods such as those that are based on adaptive control algorithms, fuzzy logic, and neural network are recently introduced to improve the controller's robustness and accuracy. One of the novel methods in control focused by investigators is active force control (AFC) because of its high accuracy, simplicity, and effectiveness. The AFC combined by means of the classical and intelligent controller was used to vehicle's active suspension systems [17-19]. The outcomes of these researches demonstrated that the AFC scheme is more capable of declining the amplitude of unwanted vibrations of the systems. In literature, there are no study works on the practical application of the AFC strategy to control the undesired vibration of a helicopter seat directly. Ahmadi *et al.* performed simulation works on the AFC scheme application to control the vertical movement of aircrew seats by integrating crude approximation technique and iterative learning (IL) [20]. The objective of the current research is to depict a novel robust control method of an active suspension system for controlling the vertical vibration of the helicopter pilot seat employing an AFC-based. In addition, implementing intelligent methods, i.e., fuzzy logic (FL), artificial neural network (ANN), and IL techniques for the computation of the estimated mass in the AFC scheme design and investigate to enhance the performance of the proposed active suspension system by simulation platform. Then, the results of the proposed schemes, namely AFCANN, AFCIL, and AFCFL, are compared together.

2. Methodology

As mentioned before, several approaches are available to cancel harmful helicopter vibrations. The present study focuses on the second approach by hybridizing AFC to seat suspension. The design steps of the controller are implied in the continue.
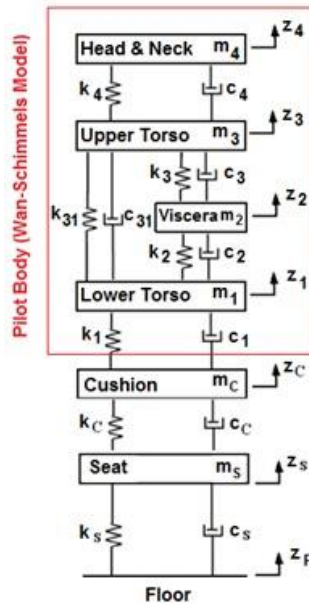

Fig. 1: The schematic of the system dynamic model

Firstly, the dynamic modeling of the vibrating system (seat and cushion plus pilot body) has been demonstrated in this section. Next, natural frequencies of the selected ultra-light helicopter structure as a case study are illustrated. Then, the AFC technique is explained. Moreover, the selected controller and actuator for the AFC technique are described. Finally, the performance of proposed control schemes is discussed based on simulation results.

2.1. System Dynamic Modeling

The schematic of the dynamic system model is illustrated in Fig. (1). As can be seen in this figure, for modeling the vibration behavior of the pilot body, the Wan-Schimmels lumped model [34] was employed. The model contains Head & Neck, Upper Torso, Viscera, and Lower Torso. The helicopter pilot seat suspension parameters include mass, stiffness, and damping constants of are listed in Table 1.

Based on Newton's Second Law and Fig. (1), the mathematical equations were derived as:

$$-c_S(\dot{z}_S-\dot{z}_F)-k_S(z_S-z_F)+c_C(\dot{z}_C-\dot{z}_S)+k_C(z_C-z_S)+F_{Floor}=m_S\ddot{z}_s \tag{1}$$

$$-c_C(\dot{z}_C-\dot{z}_S)-k_C(z_C-z_S)+c_1(\dot{z}_1-\dot{z}_C)+k_1(z_1-z_C)=m_C\ddot{z}_C \tag{2}$$

$$-c_1(\dot{z}_1-\dot{z}_C)-k_1(z_1-z_C)+c_2(\dot{z}_2-\dot{z}_1)+k_2(z_2-z_1)+c_{31}(\dot{z}_3-\dot{z}_1)+k_{31}(z_3-z_1)=m_1\ddot{z}_1 \tag{3}$$

$$-c_2(\dot{z}_2-\dot{z}_1)-k_2(z_2-z_1)+c_3(\dot{z}_3-\dot{z}_2)+k_3(z_3-z_2)=m_2\ddot{z}_2 \tag{4}$$

$$-c_3(\dot{z}_3-\dot{z}_2)-k_3(z_3-z_2)-c_{31}(\dot{z}_3-\dot{z}_1)-k_{31}(z_3-z_1)+c_4(\dot{z}_4-\dot{z}_3)+k_4(z_4-z_3)=m_3\ddot{z}_3 \tag{5}$$

$$-c_4(\dot{z}_4-\dot{z}_3)-k_4(z_4-z_3)=m_4\ddot{z}_4 \tag{6}$$

Table 1. The helicopter pilot seat suspension parameters [34 and 35]

Element	m (kg)	k (Nm^{-1})	c (Nsm^{-1})
S	15	41	148299
C	1	390	47700
1	36	49340	2475
2	5.5	20000	330
3	15	10000	200
4	5.17	134400	250
31	---	192000	909.1

2.2. Modal Analysis of Helicopter Structure

The helicopter structure was modeled in the ANSYS software in order to calculate its natural frequencies. The natural frequencies of the first six modes are zero. In other words, the first six

modes are rigid body modes [20]. The natural frequencies of seventh to twenty-six mode shapes are listed in Table 2. The detail about mode shapes is discussed in Ahmadi *et al.* (2016).

Table 2. The mode shapes and natural frequencies of the studied helicopter

Mode Shape	Frequency(Hz)	Mode Shape	Frequency(Hz)
7	6.581	17	31.161
8	7.293	18	31.640
9	8.159	19	32.747
10	9.643	20	34.571
11	9.836	21	37.338
12	11.610	22	37.413
13	13.605	23	41.052
14	14.894	24	48.125
15	18.641	25	48.760
16	22.251	26	58.642

2.3. Active force control

The AFC theory was firstly established by Burdess and Hewit to increase the robustness and stability of a robot control system in the presence of known or unknown disturbances[21]. The AFC can compensate actuated force by calculating disturbance; thus the stability and the accuracy will be increased. Where internal disturbances weight variation of the pilot, electrical noises, and friction in the actuator has been considered, the external disturbance was helicopter cabin vibration. The main concept of the AFC technique is shown in Fig. (2).
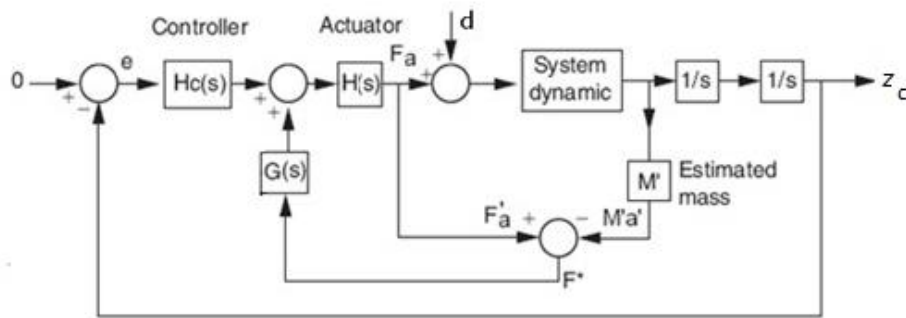

Fig. 2: A representation block diagram of an AFC technique

Regards to Fig. (2) and Newton Second Law, we have:

$$F^* = F'_a - M'a'$$

(7)

where a' and F'_a are seat acceleration (in this study) and actuator force, respectively. These parameters can be calculated by acceleration and force sensors. Additionally, M' and F^* are estimated mass and compensator force, respectively. The estimated mass may be given by assuming a perfect model, crude approximation [22-24], or intelligent techniques such as hybrid intelligent [25], ANN [18, 26, 27], IL [24, 28-30], and FL [16, 31].

2.4. Selection of controller for AFC technique

In this study, the outer loop controller was designed via a PID controller. The PID controller is suitable for systems that have low-frequency noise and disturbances. The transfer function of the PID controller is given as:

$$G_c(s) = K_P + \frac{K_I}{s} + K_D s \tag{8}$$

where K_P, K_D and K_I are the proportional, derivative, and integral parameters, respectively. After the tuning process with the Ziegler-Nichols method, these parameters were obtained as: $K_P = 120$ $K_I = 0$ and $K_D = 20$. It is executed by setting the K_D and the K_I gains to zero. Then, the K_P increased to reach a stable oscillation named ultimate gain, K_u. Based on the K_u and oscillation period, T_u, the PID gains were obtained as:

$K_P = 0.6k_u$ $K_I = {T_u}/{2}$ and $K_D = {T_u}/{8}$. The tuning process was done two times for all schemes; firstly, just with the PID, and secondly by the PID and the AF C schemes (AFCANN, AFCIL, and AFCFL).

2.5. Selection of the actuator for the AFC technique

A linear electrical motor has been chosen as the actuator. The actuated force has a direct relationship to electrical current. So, the force can be stated as:

$$F = K_{fn} I \tag{9}$$

The linear motor transfer function is given as:

$$H(s) = K_{fn} s \tag{10}$$

where K_{fn} is motor force constant which was considered 360 NA^{-1}. "I" is an electrical current. The suggested linear electrical model is Tritex Actuator made by ELEXAR Company. In addition, the transfer function G(s) will be G(s) $=(1/K_{fn})s$ which G(s) is the inverse of the actuator.

3. Simulation

Computer simulations were performed using the MATLAB/Simulink environment to verify the proposed control schemes. Simulation of Helicopter Cabin Floor Vibrations and suggested Control Schemes are explained in this section.

3.1. Simulation of Helicopter Cabin Floor Vibrations

To simulate the helicopter cabin floor displacement transmitted to the helicopter seat and pilot body, first, an acceleration signal of 1/rev, 2/rev, and 4/rev harmonics of main rotor speed was generated. The fundamental frequency was set at 8.33 Hz to correlate with the studied helicopter main rotor speed. The amplitude of each harmonic was set to 0.147 g and the level of overall sinusoidal acceleration was 0.18 g [15]. Next, the random acceleration signal that covered the natural frequencies of the studied helicopter structure in the range from 4 to 50 Hz was produced. The level of overall random acceleration was kept at 0.08 g. Subsequently, the generated sinusoidal and random acceleration signals were converted to displacement. Finally, sinusoidal and random displacement profiles were combined.

3.2. The AFCANN Control Scheme

As mentioned previously, mass estimation in the AFC scheme is the key part, so the ANN was chosen for this prediction. Fig. (3) represents the block diagram of the AFCANN scheme. In this method, a feed-forward back-propagation ANN (FFBP) structure with a single hidden layer with ten neurons was employed to compute the estimated mass. The input is error signal, and the output is the estimated mass. The topology of the established ANN model is illustrated in Fig. (4). The output/input relationship of a neuron describes by the general equation is as follows:

$$y = f \left(\sum_{i=1}^{m} w_i I_i + b \right) \tag{11}$$

where $f(\ )$, w, and b are sigmoid function, weight, and bias, respectively. The sigmoid function is given as:
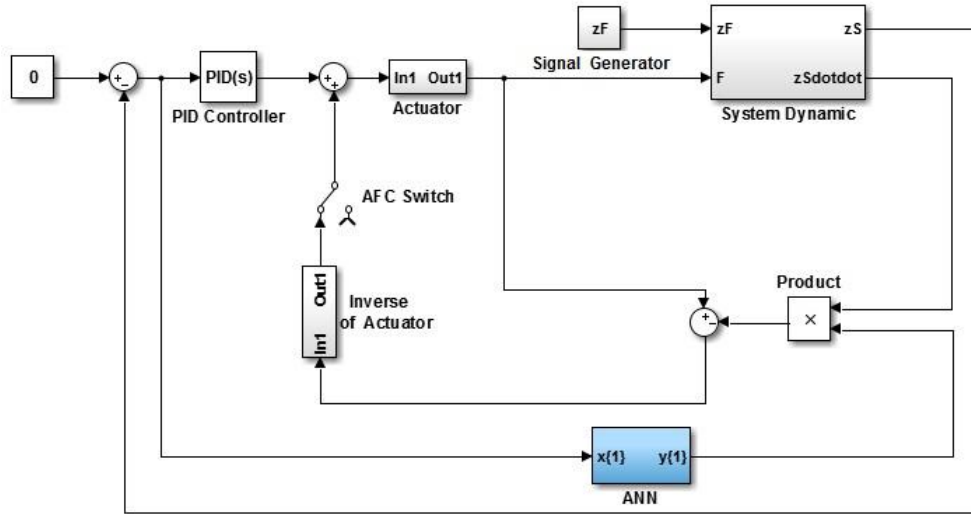
$$f(x) = \frac{1}{1 + e^{-x}} \tag{12}$$

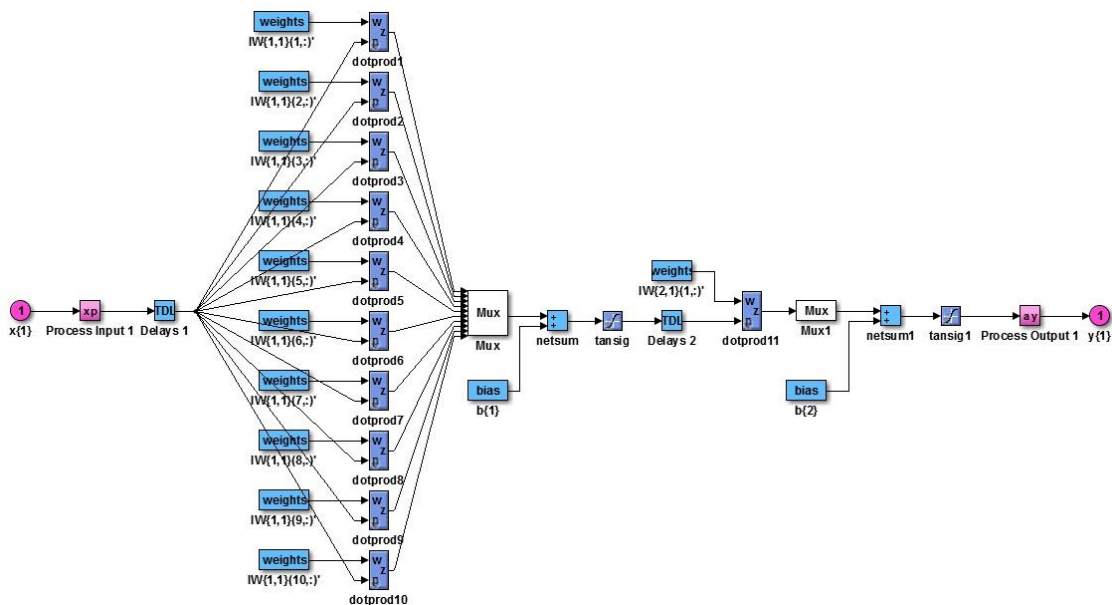**Fig. 3**: The block diagram of the AFCANN control scheme

Fig. 4: The topology of the established ANN model

The Levenberg-Marquardt Algorithm was used as a learning algorithm. Sigmoid was employed as Activation Function, and weights were adjusted by software. The best architecture of ANN was reached by one hidden layer, and the correlation ratio is 92.23%. Data split into three sub-set for training (60%), testing (20%) and cross-validation (20%). The excitation signal is the acceleration of the seat pan.

3.3. The AFCIL Control Scheme

In addition to the ANN, the AFC was equipped with the IL algorithm established by Arimoto to estimate the mass. Fig. (5) demonstrates the block diagram of the AFCIL approach. The mathematical equation of Arimoto's iterative algorithm is like the classical PID controller and applies the proportional (φ), integral (ψ), and derivative (Γ) learning parameters [32]. The PID-type IL algorithms can be exploited as follows:

$$PID - type: M'_{k+1} = M'_k + \left(\varphi + \psi \int dt + \Gamma \frac{d}{dt}\right) e_k \tag{13}$$

where M'_k and M'_{k+1} are the current and next step values of the estimated mass, respectively, and e_k is the current error. In this research, the crude approximation as an initial value of the estimated mass was utilized, which was considered 0.27 kg. The tuning process of IL coefficients was done, and parameters were obtained as $\varphi=1$, $\psi=1$, $\Gamma=1$. The stability and minimum overshoot of response were criteria of the tuning step. The block diagram of the IL algorithm is exemplified in Fig. (6).
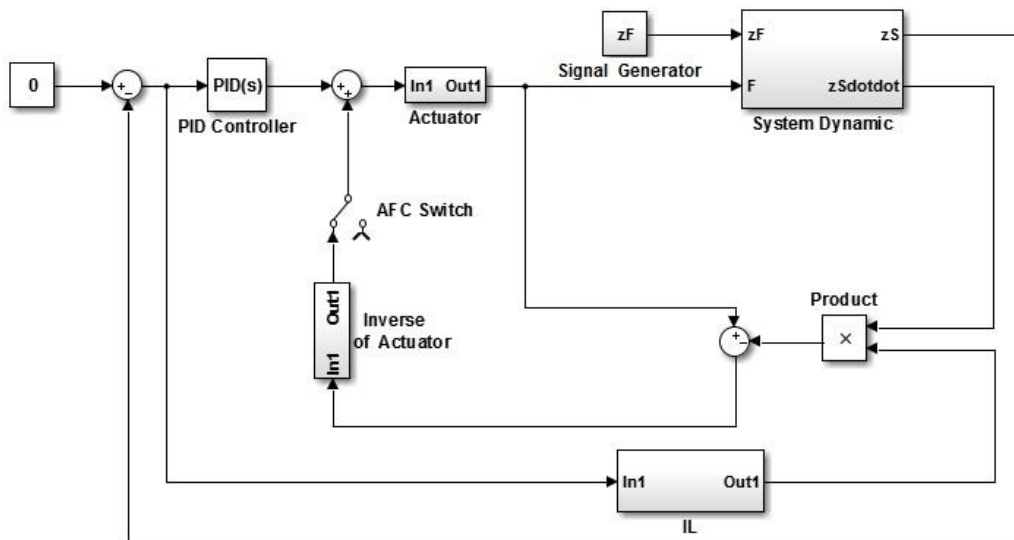

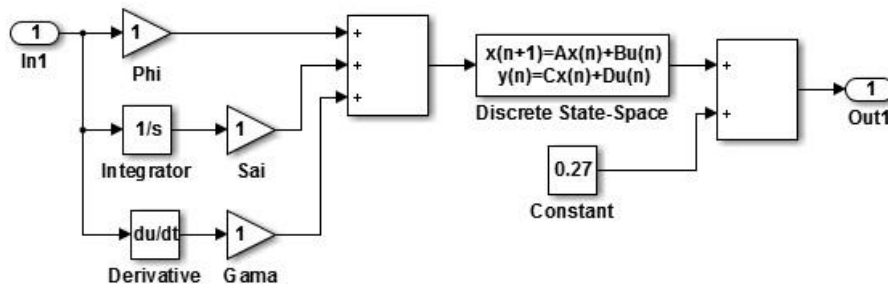**Fig. 5:** The block diagram of the AFCIL control scheme

Fig. 6: The block diagram of the established IL algorithm

3.4. The AFCFL Control Scheme

FL technique is an intelligent technique that is presented by Zadeh based on the human inference system. It can be applied for estimating, decision making, multivariable adaptive control, etc. [33]. As a third approach for estimating the mass value in the AFC, the FL was chosen and integrated into that. Fig. (7) reveals the block diagram of the AFCFL scheme. In this scheme, the Mamdani engine was employed as an inference system to calculate output which is estimated mass. The membership functions representing the inputs (the error signal (seat displacement) and the derivative of the error signal (or seat velocity) and output (estimated mass) are unveiled in Fig. (8). As can be observed in this figure, the input variables were classified into five sections as triangular membership functions using Positive Small (PS), Positive Large (PL), Zero (Z), Negative Large (NL) and Negative Small (NS) based on linguistic variables. Also, the output variable was classified into three sections using Large (L), Medium (M), and Small (S) based on linguistic variables. Same as inputs, the triangular membership function was selected for output. The fuzzy rule base of the AFCFL scheme is summarized in Table 3. Seat displacement and seat velocity considered as inputs must impose the estimated mass to have minimum variation and overshoot in the response of the seat. For example, positive small seat displacement and small negative value of seat velocity indicate the medium value of estimated mass to show good performance of the seat suspension.
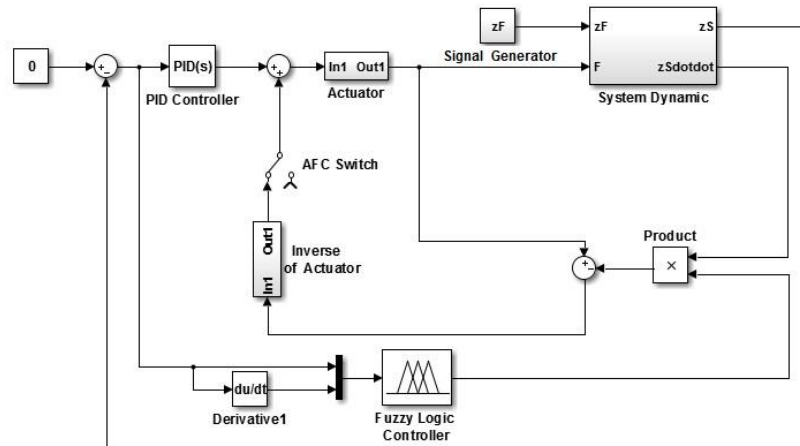

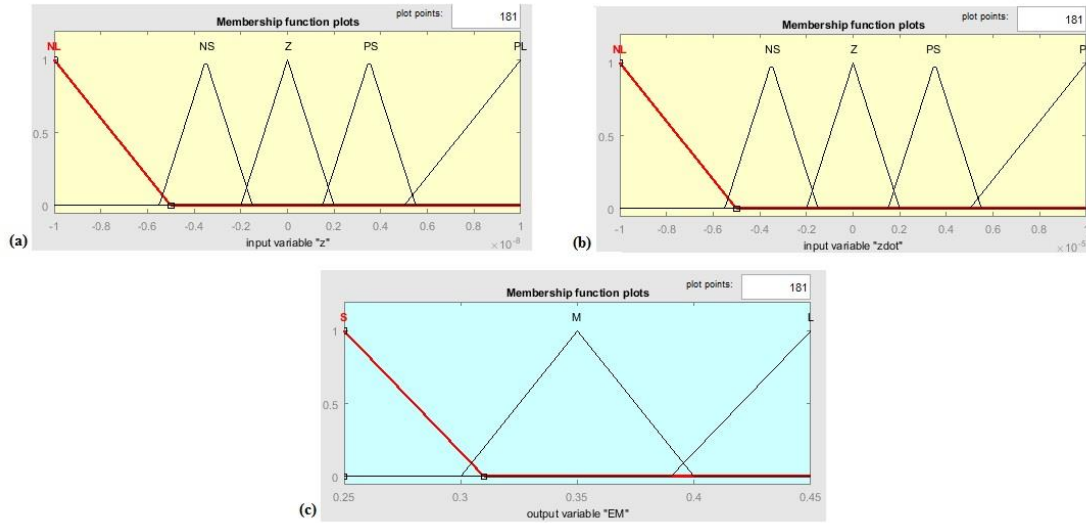**Fig. 7**: The block diagram of the AFCFL control scheme

Fig. 8. The membership functions (a) error signal (b) Derivative of the error signal (c) estimated mass

Table 3: The fuzzy rule base

Seat Displacement	Seat Velocity				
	NL	NS	Z	PS	PL
NL	---	---	L	---	---
NS	---	M	---	M	---
Z	S	---	S	---	S
PS	---	M	---	M	---
PL	---	---	L	---	---

4. Results and Discussion

To validate the performance of the designed controllers, the simulation results of the proposed control schemes are shown in this part and compared with the PID control scheme and uncontrolled system. Initially, pilot head displacement and acceleration have been investigated. The charts in the frequency and time domains are revealed as a line, respectively.

The pilot head displacement in the time domain is shown in Fig. (9). As can be found in this figure, the maximum displacement of the head in the time domain without the controller and with the PID scheme is from the order of 10^{-4} but using of proposed control schemes reduced this value down to the order of 10^{-10}.
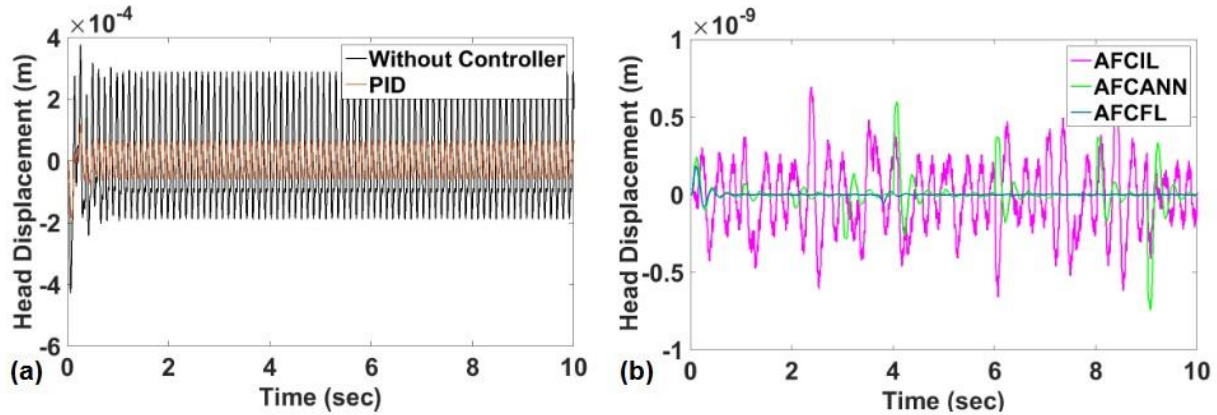
Fig. 9. The pilot head displacement in the time domain (a) without controller and with the PID scheme (b) with proposed control schemes

Moreover, the pilot head displacement in the frequency domain is illustrated in Fig. (10). Note that the AFCFL scheme is not seen well in this figure because of its small magnitude. As can be distinguished in this figure, the maximum displacement of the head in the frequency domain has occurred in the 1/rev and 2/rev harmonics of the main rotor fundamental frequency, respectively. The maximum order of head displacement without the controller and with the PID scheme is from the order of 10^{-4} though the maximum order of head displacement is from the order of 10^{-11} by using the AFCANN and the AFCIL schemes and from the order of 10^{-12} via the AFCFL scheme. The maximum displacement of the head has occurred in the frequency range of less than 1/rev in all proposed control schemes.
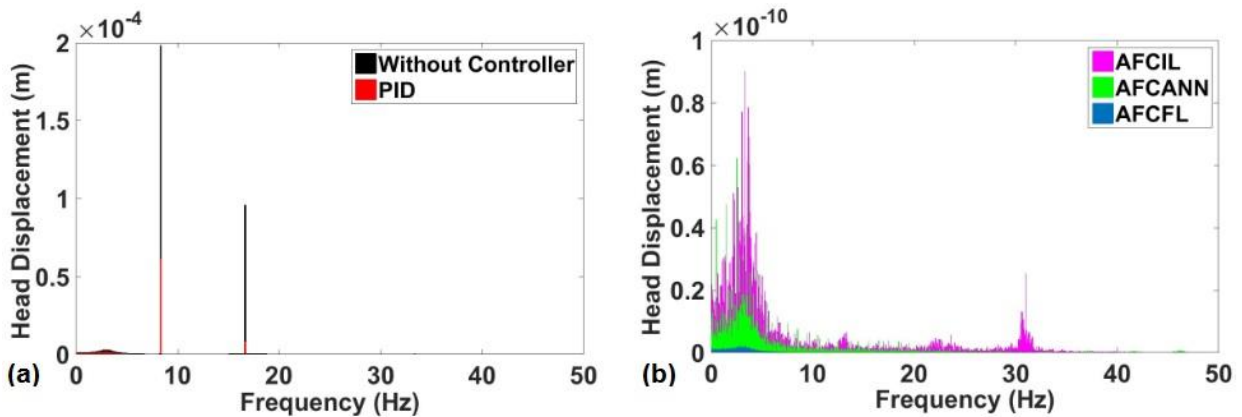

Fig. 10. The pilot head displacement in the frequency domain: (a) without the controller and with the PID scheme (b) with proposed control schemes

Furthermore, Fig. (11) presents the pilot head acceleration in the time domain. As can be seen, the maximum head acceleration in the time domain without the controller and with the PID scheme is from the order of 10^{-1}, but employing the AFCANN and the AFCIL schemes decrease this value to the order of 10^{-7}. Similarly, this value was reduced to the order of 10^{-8} by means of the AFCFL scheme.
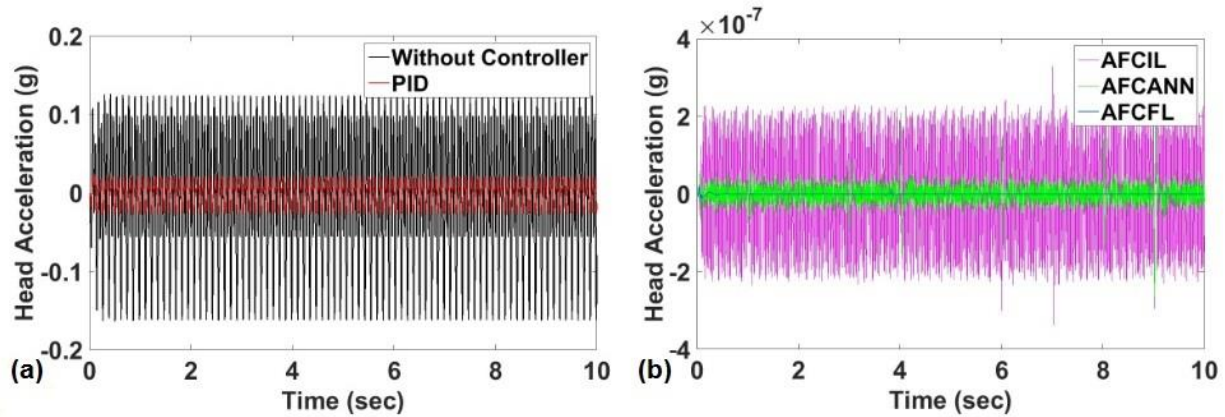
Fig. 11. The pilot head acceleration in the time domain (a) without the controller and with the PID scheme (b) with proposed control schemes

The pilot head acceleration in the frequency domain is unveiled in Fig. (12). Remind that the AFCFL scheme is not seen well again in this figure because of its small magnitude. The notable point in this figure is the maximum head acceleration that has occurred in the 2/rev, 1/rev, and 4/rev harmonics, respectively. The maximum order of head acceleration without the controller and with the PID scheme is from the order of 10^{-1} and 10^{-2}, respectively. Although the maximum order of head acceleration is from the order of 10^{-8}, 10^{-9}, and 10^{-11} by applying the AFCIL, AFCANN, and AFCFL schemes, respectively. The maximum head acceleration has been generated in the frequency range of 40-50 Hz in the AFCANN scheme, 30-35 Hz in the AFCIL scheme and less than 1/rev in the AFCFL scheme. Therefore, the pilot head displacement and acceleration are controlled effectively by utilizing each of the proposed control schemes in comparison to the uncontrolled system and use of the PID scheme. Also, the AFCFL scheme has shown superior results. In addition to the maximum order of head displacement and acceleration, similar results for the seat, cushion, and other parts of the pilot body are listed in Table 4 and Table 5 in the time domain, and in Table 6 and Table 7 in the frequency domain.
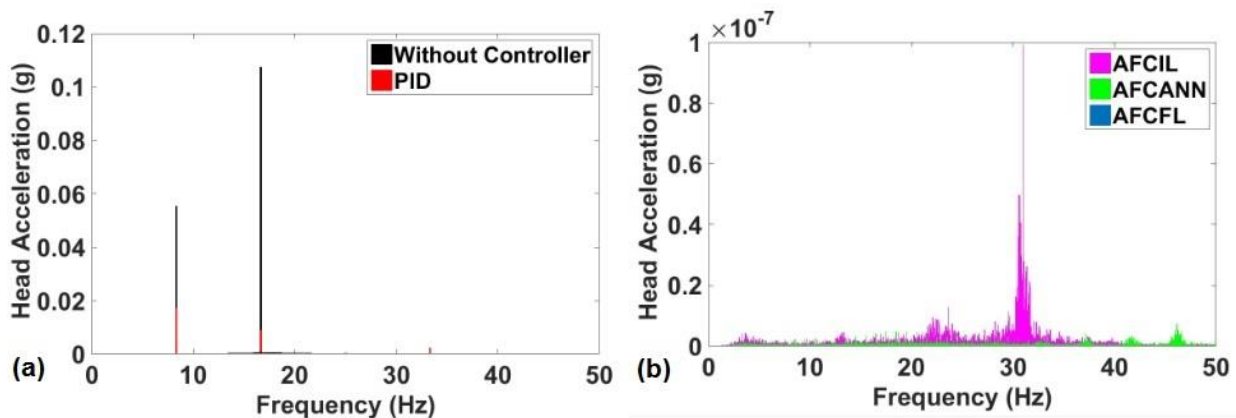

Fig. 12. The pilot head acceleration in the frequency domain (a) without the controller and with the PID scheme (b) with proposed control schemes

Table 4: The maximum order of displacement in the time domain

Control Scheme	Maximum order of displacement (m)
Without Controller	10^{-4}
PID	10^{-4}
AFCANN	10^{-9} (Seat and Cushion), 10^{-10} (Pilot Body)
AFCIL	10^{-9} (Seat and Cushion), 10^{-10} (Pilot Body)
AFCFL	10^{-10}

Table 5: The maximum order of acceleration in the time domain

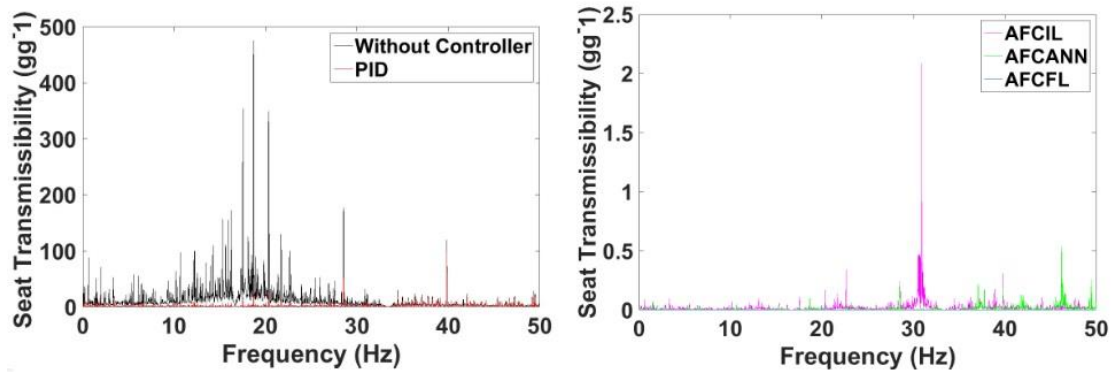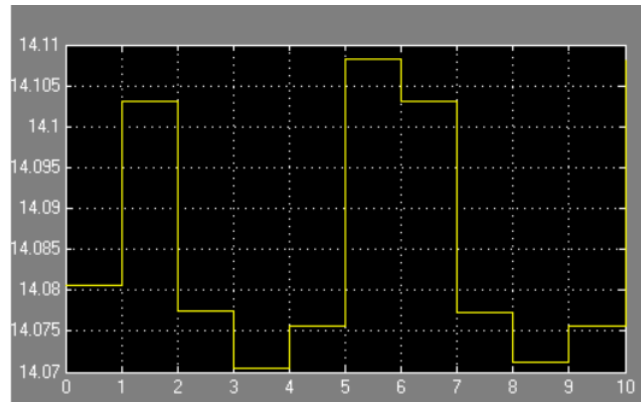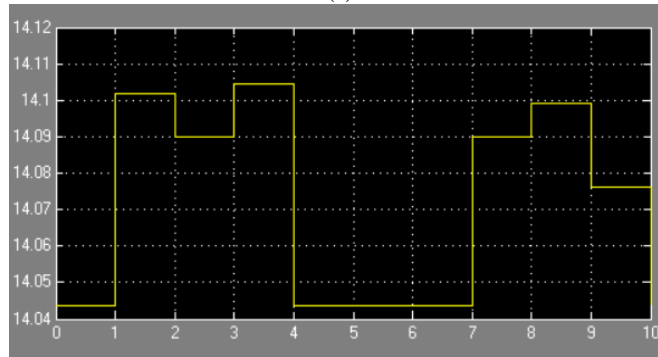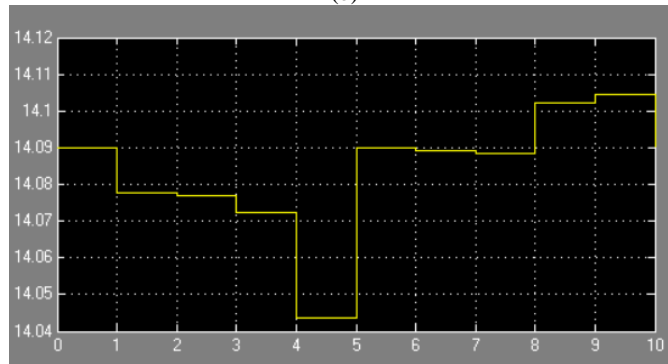| Control Scheme	Maximum order of acceleration (g)					
	Seat	Cushion	Lower Torso	Viscera	Upper Torso	Head
Without Controller	10^{-1}	10^{-1}	10^{-2}	10^{-2}	10^{-2}	10^{-1}
PID	10^{-1}	10^{-2}	10^{-2}	10^{-2}	10^{-2}	10^{-2}
AFCANN	10^{-3}	10^{-4}	10^{-5}	10^{-7}	10^{-7}	10^{-7}
AFCIL	10^{-3}	10^{-4}	10^{-5}	10^{-7}	10^{-7}	10^{-7}
AFCFL	10^{-3}	10^{-4}	10^{-5}	10^{-7}	10^{-7}	10^{-8}

Fig. 13. The seat transmissibility in the frequency domain (a) without the controller and with the PID scheme (b) with the AFCANN and AFCIL control schemes

(a)

(b)

(c)

Fig. 14. Estimated mass with various algorithms (a) With the Neural Network (b) with the Iterative Learning and (c) with the Fuzzy Logic

Table 6: The maximum order of displacement in the frequency domain

Control Scheme	Maximum order of displacement (m)
Without Controller	10^{-4}
PID	10^{-4} (Seat), 10^{-5} (Cushion and Pilot Body)
AFCANN	10^{-11}
AFCIL	10^{-11}
AFCFL	10^{-14} (Seat), 10^{-12} (Cushion and Pilot Body)

Table 7: The maximum order of acceleration in the frequency domain

Control Scheme	Maximum order of acceleration (g)					
	Seat	Cushion	Lower Torso	Viscera	Upper Torso	Head
Without Controller	10^{-1}	10^{-1}	10^{-2}	10^{-2}	10^{-2}	10^{-1}
PID	10^{-2}	10^{-2}	10^{-2}	10^{-2}	10^{-2}	10^{-2}
AFCANN	10^{-5}	10^{-6}	10^{-7}	10^{-8}	10^{-8}	10^{-9}
AFCIL	10^{-5}	10^{-6}	10^{-7}	10^{-8}	10^{-8}	10^{-8}
AFCFL	10^{-9}	10^{-9}	10^{-10}	10^{-10}	10^{-11}	10^{-11}

Finally, the seat acceleration transmissibility has been investigated. Fig. (13) shows the seat acceleration transmissibility diagram. As can be known, by employing the AFCIL, AFCANN, and AFCFL schemes, the seat acceleration transmissibility was reduced to 2.09, 0.54, and 2×10^{-3}, respectively. Note that the AFCFL scheme is not seen well in this figure because of its small magnitude). These results demonstrate the effectiveness of the proposed control schemes and confirm the superiority of the AFCFL control scheme. Besides, the pilot riding comfortability may be increased based on ISO 2631-1, because critical vibration for the spinal column is between 4 to 8 Hz while pilot vibration was reduced in this range by the AFC schemes (Fig. (10), Fig. (12), and Fig. (13)). Whereas the performance of algorithms in the estimation of mass affects controller accuracy, these values are exemplified in Fig. (14). As can be seen, the AFCFL has more variations at the same time.

5. Conclusion

Reduction of body displacement and acceleration of helicopter pilot may diminish the risk of generating spine column and neck physical problems. Seat suspension can block harmful and unwanted vibrations. In this paper, a novel controller utilizing the AFC has been successfully developed and simulated for the helicopter pilot seat suspension system. Three control schemes were focused on hybridizing by the AFC: ANN, IL algorithm, and FL called AFCANN, AFCIL and, AFCFL, respectively. The AFC-based method is found to be computationally simple and efficient and yet produce accurate and robust even in the attendance of different disturbances. The pilot head displacement and acceleration and also seat acceleration transmissibility were selected as target variables. The simulation results demonstrated that for given parameters, the proposed AFCFL enhances the scheme performance compared to the PID controller, uncontrolled, AFCANN, and AFCIL. Future work is aimed to develop helicopter pilot seat suspension as a test rig based on current simulation achievements to evaluate the performance of the selected scheme practically.

Funding

Declaration of conflicting interests

The authors declare that there is no conflict of interest in preparing this paper.

References

[1] N.A.C. Branco, E. Rodriguez, The vibroacoustic disease--an emerging pathology, Aviation, space, and environmental medicine, 70 (1999) A1-A6.

[2] Y. Chen, V. Wickramasinghe, D.G. Zimcik, Development of adaptive helicopter seat systems for aircrew vibration mitigation, in: Active and Passive Smart Structures and Integrated Systems 2008, International Society for Optics and Photonics, 2008, pp. 69280N.

[3] P.C. Chen, I. Chopra, Wind tunnel test of a smart rotor model with individual blade twist control, Journal of Intelligent Material Systems and Structures, 8 (1997) 414-425.

[4] F.K. Straub, H.T. Ngo, V. Anand, D.B. Domzalski, Development of a piezoelectric actuator for trailing edge flap control of full scale rotor blades, Smart materials and structures, 10 (2001) 25.

[5] K. Nguyen, M. Betzina, C. Kitaplioglu, Full-Scale Demonstration of Higher Harmonic Control for Noise and Vibration Reduction on the XV-15 Rotor, Journal of the American Helicopter Society, 46 (2001) 182-191.

[6] S.B. Choi, J.H. Choi, M.H. Nam, C.C. Cheong, H. Lee, A semi-active suspension using ER fluids for a commercial vehicle seat, Journal of Intelligent Material Systems and Structures, 9 (1998) 601-606.

[7] S.-B. Choi, M.-H. Nam, B.-K. Lee, Vibration control of a MR seat damper for commercial vehicles, Journal of intelligent material systems and structures, 11 (2000) 936-944.

[8] P. De Man, P. Lemerle, P. Mistrot, J.-P. Verschueren, A. Preumont, An investigation of a semiactive suspension for a fork lift truck, Vehicle System Dynamics, 43 (2005) 107-119.

[9] C. Liangbin, C. Dayue, A two-stage vibration isolation system featuring an electrorheological damper via the semi-active static output feedback variable structure control method, Journal of Vibration and Control, 10 (2004) 683-706.

[10] C. Park, D. Jeon, Semiactive vibration control of a smart seat with an MR fluid damper considering its time delay, Journal of intelligent material systems and structures, 13 (2002) 521-524.

[11] S.J. McManus, K.S.t. Clair, P.E. Boileau, J. Boutin, S. Rakheja, Evaluation of vibration and shock attenuation performance of a suspension seat with a semi-active magnetorheological fluid damper, Journal of Sound and Vibration, 253 (2002) 313-327.

[12] Y.-T. Choi, N.M. Wereley, Biodynamic response mitigation to shock loads using magnetorheological helicopter crew seat suspensions, Journal of aircraft, 42 (2005) 1288-1295.

[13] G.J. Hiemenz, W. Hu, N.M. Wereley, Semi-active magnetorheological helicopter crew seat suspension for vibration isolation, Journal of Aircraft, 45 (2008) 945-953.

[14] Y. Chen, V. Wickramasinghe, D. Zimcik, Development of adaptive seat mounts for helicopter aircrew body vibration reduction, Journal of Vibration and Control, 15 (2009) 1809-1825.

[15] Y. Chen, V. Wickramasinghe, D.G. Zimcik, Development of adaptive helicopter seat for aircrew vibration reduction, Journal of Intelligent Material Systems and Structures, 22 (2011) 489-502.

[16] M. Mailah, N.I.A. Rahim, Intelligent active force control of a robot arm using fuzzy logic, in: 2000 TENCON proceedings. Intelligent systems and technologies for the new millennium (Cat. No. 00CH37119), IEEE, 2000, pp. 291-296.

[17] G. Priyandoko, M. Mailah, Simulation of suspension system with adaptive fuzzy active force control, To all Intelligent Active Force Control Research Group, 30 (2007).

[18] G. Priyandoko, M. Mailah, H. Jamaluddin, Vehicle active suspension system using skyhook adaptive neuro active force control, Mechanical systems and signal processing, 23 (2009) 855-868.

[19] K. Rajeswari, P. Lakshmi, Simulation of suspension system with intelligent active force control, in: 2010 International Conference on Advances in Recent Technologies in Communication and Computing, IEEE, 2010, pp. 271-277.

[20] S. Ahmadi, M. Gohari, M. Tahmasebi, Intelligent active force control of a helicopter seat suspension using iterative learning algorithm, in: 2016 6th International Conference on Computer and Knowledge Engineering (ICCKE), IEEE, 2016, pp. 30-35.

[21] J.S. Burdess, J.R. Hewit, An active method for the control of mechanical systems in the presence of unmeasurable forcing, Mechanism and Machine Theory, 21 (1986) 393-400.

[22] H. Jahanabadi, M. Mailah, h. M.d., Active control of a robotic arm with pneumatic artificial muscle actuator, in: Proceedings of third South East Asian Technical Universities Consortium Symposium, 2009, pp. 417-420.

[23] M. Mailah, Intelligent active force control of a rigid robot arm using neural network and iterative learning algorithms, in, University of Dundee, 1998.

[24] M. Tahmasebi, M. Mailah, M. Gohari, R. Abd Rahman, Vibration suppression of sprayer boom structure using active torque control and iterative learning. Part I: Modelling and control via simulation, Journal of Vibration and Control, 24 (2018) 4689-4699.

[25] S.B. Hussein, H. Jamaluddin, M. Mailah, A.M.S. Zalzala, A hybrid intelligent active force controller for robot arms using evolutionary neural networks, in: Proceedings of the 2000 Congress on Evolutionary Computation. CEC00 (Cat. No. 00TH8512), IEEE, 2000, pp. 117-124.

[26] C.K. Loo, R. Mandava, M.V.C. Rao, A hybrid intelligent active force controller for articulated robot arms using dynamic structure neural network, Journal of Intelligent and Robotic Systems, 40 (2004) 113-145.

[27] M. Tahmasebi, R.A. Rahman, M. Mailah, M. Gohari, Roll movement control of a spray boom structure using active force control with artificial neural network strategy, Journal of low frequency noise, vibration and active control, 32 (2013) 189-201.

[28] L.C. Kwek, E.K. Wong, C.K. Loo, M.V.C. Rao, Application of active force control and iterative learning in a 5-link biped robot, Journal of Intelligent and Robotic Systems, 37 (2003) 143-162.

[29] M. Mailah, H.M. Hooi, S. Kazi, H. Jahanabadi, Practical active force control with iterative learning scheme applied to a pneumatic artificial muscle actuated robotic arm, International Journal of Mechanics, 1 (2012) 88-96.

[30] M. Tahmasebi, M. Gohari, M. Mailah, R. Abd Rahman, Vibration suppression of sprayer boom structure using active torque control and iterative learning. Part II: Experimental implementation, Journal of Vibration and Control, 24 (2018) 4740-4750.

[31] H. Jahanabadi, M. Mailah, M.-M. Zain, H.M. Hooi, Active force with fuzzy logic control of a two-link arm driven by pneumatic artificial muscles, Journal of Bionic Engineering, 8 (2011) 474-484.

[32] S. Arimoto, S. Kawamura, F. Miyazaki, Bettering operation of robots by learning, Journal of Robotic systems, 1 (1984) 123-140.

[33] L.A. Zadeh, Fuzzy sets. Information and control, in: Fuzzy sets, World Scientific, 1965, pp. 338-353.